PHYSICAL REVIEW B VOLUME 46, NUMBER 22 1 DECEMBER 1992-II

Polarization study and crystal-field analysis of the laser-selective excitation spectra of Ho^{3+} ions in CaF_2 and SrF_2 crystals

Marjorie Mujaji, G. D. Jones, and R. W. G. Syme
Department of Physics and Astronomy, University of Canterbury, Christchurch, New Zealand

(Received 30 June 1992)

The polarized fluorescence of a total of 12 Ho^{3+} ion centers present in CaF_2- and SrF_2-type crystals and having a variety of Ho^{3+} ion symmetries has been analyzed to give possible model assignments. In contrast to the earlier results for SrF_2:Er^{3+}, which has a dominant trigonal symmetry center, the principal center in SrF_2:Ho^{3+} is determined to have tetragonal symmetry. Crystal-field analyses are reported for both the tetragonal and trigonal symmetry centers, together with fluorescence-lifetime data for these centers.

I. INTRODUCTION

Polarization of laser-selective excitation fluorescence spectra of rare-earth ions in CaF_2-type crystals can help in determining center symmetries and assigning group symmetry labels to particular energy levels. Laser-selective excitation is a well established method for identifying lines of multicenter spectra and has been used, in particular, to characterize the two principal single Ho^{3+} centers found in CaF_2:Ho^{3+} crystals.[1] Tetragonal (C_{4v}) or trigonal (C_{3v}) symmetry sites in the CaF_2 structure have three or four possible orientations, respectively, of the principal axis of symmetry of the centers. Some orientations of these centers are preferentially excited by polarized laser light incident along a crystal symmetry direction, giving a net polarized emission. Such polarization determinations of center symmetries have been made with varying success for Er^{3+} ions in CaF_2,[2] and SrF_2,[3] and for Pr^{3+} ions in CaF_2 and SrF_2.[4]

In this paper we present detailed polarization studies of the spectra of Ho^{3+} ions in CaF_2 crystals, in CaF_2 crystals containing 1% of SrF_2 or BaF_2, in SrF_2 crystals and in SrF_2 crystals containing 1% of CaF_2 or BaF_2, and use them to propose specific model configurations of the various centers present. In CaF_2:Ho^{3+} it was established by Seelbinder and Wright[1] that there are two principal centers (labeled by them *A* and *B* sites), which were assigned as having C_{4v} and C_{3v} symmetry, respectively, and we report polarization measurements which confirm these assignments.[5] Assignment of the different spectral transitions to either *A* or *B* centers has been confirmed recently[6] on the basis of the respective center lifetimes.

We also report laser-selective excitation measurements of four modified centers present in mixed CaF_2:1% SrF_2 and CaF_2:1% BaF_2 crystals, both containing Ho^{3+}, arising from replacement of one of the 12 nearest-neighbor Ca^{2+} ions by either a Sr^{2+} or Ba^{2+} ion.[7] The 1% concentration of dopant alkaline-earth cations was chosen to give centers having just one dopant cation a high concentration relative to those having more than one such dopant cation. The substitution by either Sr^{2+} or Ba^{2+} ions is found here to yield one center of C_{4v} symmetry (with an on-axis placement of the dopant alkaline-earth cation) and one of lower C_s symmetry (with an off-axis placement of the dopant alkaline-earth cation) for each of the mixed crystal systems as indicated in Fig. 1. For the lower symmetry centers, there are observed splittings of those transitions involving doublet levels (γ_5 symmetry under C_{4v}) and the transition polarizations are consistent

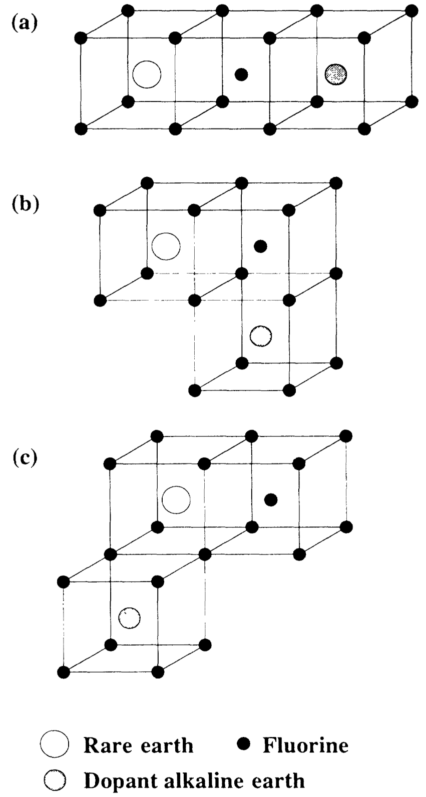

FIG. 1. Proposed modified C_{4v} center configurations obtained by introduction of a different alkaline-earth cation in the configuration of the regular C_{4v} center. (a) The on-axis modified C_{4v} symmetry center, (b) the off-axis (100) plane C_s symmetry center, and (c) the off-axis (110) plane C_s symmetry center.

with a C_s site symmetry.

In SrF_2 crystals containing rare-earth ions there is a changeover of symmetry of the principal center present as one goes along the rare-earth series, and this occurs in the vicinity of Dy^{3+} and Ho^{3+}.[8] The electron-paramagnetic-resonance (EPR) spectra of rare-earth ions in SrF_2 crystals are characterized by the observation of predominantly tetragonal symmetry centers for rare-earth ions in the first part of the rare-earth series and both trigonal and cubic symmetry centers for rare-earth ions in the latter part.[8] SrF_2 crystals containing Ce^{3+},[8] Nd^{3+},[9] and Sm^{3+} (Ref. 10) ions all have only tetragonal symmetry centers in their EPR spectra, SrF_2 crystals containing Gd^{3+} (Ref. 11) and Dy^{3+} (Ref. 12) ions have both tetragonal and trigonal symmetry centers present, while those containing Er^{3+} (Ref. 8) and Yb^{3+} (Ref. 13) ions have both trigonal and cubic symmetry centers. For SrF_2 crystals containing 0.1% Ho^{3+}, EPR results indicate the presence of a principal trigonal symmetry center, whose EPR resonances occur at both 9.5 and 35 GHz through mechanisms discussed in detail by Ranon and Lee.[14]

Published spectroscopic results for SrF_2:Ho^{3+} include an argon laser excitation study of SrF_2:1% Ho^{3+},[15] which revealed three fluorescence groups, without any specific center assignments being made. Our results are of a polarized laser-selective excitation study of SrF_2:0.005% Ho^{3+} and SrF_2:0.01% Ho^{3+} crystals. The similarity of the spectral lines reported here for the principal center, both in line intensity patterns and polarization, to those of the well established tetragonal symmetry (A) center observed in CaF_2:Ho^{3+} indicates the preferential formation of a tetragonal symmetry center in SrF_2:Ho^{3+} (henceforth labeled the SrF_2 A center). Three other weaker centers are also observed and are identified as modified A centers involving nearby unintentionally introduced Ca^{2+} or Ba^{2+} ions. Two of these centers are identified as having C_{4v} symmetry Ho^{3+} sites, with associated on-axis Ca^{2+} or Ba^{2+} ions, whereas the third center is analogous to the low symmetry (C_s) CaF_2:Ho^{3+} center associated with an off-axis dopant alkaline-earth ion.[7]

Our optical spectroscopy results for SrF_2:Ho^{3+} are in marked contrast to those for SrF_2:0.05% Er^{3+} crystals, where similar investigations[3,16] revealed four centers, the strongest of which (the so-called J center) has trigonal symmetry and the three others ($N1$, $N2$ and $N3$) are modifications of this J center. Only after hydrogenation were some tetragonal symmetry Er^{3+} centers produced and these involve hydride ion charge compensation.

Our optical spectroscopy results are also in apparent disagreement with the EPR measurements that indicate the presence of only a trigonal symmetry Ho^{3+} center. Optical transitions we have assigned to a trigonal symmetry B center are quite weak, having an intensity only 2% of corresponding transitions we have assigned to the principal tetragonal (C_{4v}) symmetry A center. As the ground state and first excited state of Ho^{3+} ions in this SrF_2:Ho^{3+} A center are determined by our optical spectroscopy measurements to be crystal-field orbital singlets separated by 2.7 cm^{-1}, this C_{4v} symmetry center could have no EPR resonances at either 9.5 or 35 GHz and hence the absence of any tetragonal symmetry center resonances is explained. EPR measurements at 75 GHz, as were reported for CaF_2:Ho^{3+} crystals,[17] would be needed to detect the presence of this C_{4v} center by EPR and to confirm the observed 2.7 cm^{-1} energy-level splitting.

Optical spectroscopy measurements favor the observation of C_{4v} symmetry centers as the line strengths of optical transitions of any trigonal symmetry center, whose configuration is closer to cubic symmetry than a C_{4v} center, would be lower than those of such C_{4v} centers. Hence the measured 2% relative line strengths of the B center lines underestimate the population of the trigonal symmetry B center actually present.

II. EXPERIMENTAL

Crystals were grown by the Bridgman-Stockbarger method using a 38 kW A.D. Little rf induction furnace. CaF_2, SrF_2, and BaF_2 offcuts and 99.9% pure HoF_3 powder were used as starting materials. The crystals used for polarization studies were lowered at a rate of 2.5 mm/h, over a total growth time of 30 h and a subsequent annealing time of 3 h. Two additional SrF_2:Ho^{3+} crystals, with 0.005 and 0.1 % concentrations of Ho^{3+}, respectively, were purchased from Optovac Inc. for use as reference samples.

Apart from the use of a Spectra-Physics 2045 argon laser, the spectroscopic equipment and techniques employed were as described for the earlier CaF_2:Er^{3+} work.[2] Coumarin 540 and Rhodamine 640 dyes were appropriate for excitation of Ho^{3+}. Most spectroscopic measurements were for samples cooled to 10 K in a closed-cycle cryostat. Some 2 K measurements were obtained by immersion of the sample in superfluid helium.

All reported wave numbers are as recorded in air.

For the fluorescence-lifetime measurements, the equipment was as used for the earlier CaF_2:Pr^{3+} and SrF_2:Pr^{3+} study,[4] with the addition of a digital storage oscilloscope to record and average 256 fluorescence decay transients, as recorded by a Spex 1700 0.75 m monochromator equipped with an EMI9558QA photomultiplier tube.

III. SPECTROSCOPY OF Ho^{3+} IN CaF_2 AND SrF_2

A. Energy levels of centers having Ho^{3+} ions located in sites of C_{4v} and C_{3v} symmetry

The $4f^{10}$ configuration, appropriate for trivalent Ho^{3+} ions, has three multiplets ($^5S_2$ and $^5F_4$ in the 18 000 cm^{-1} and $^5F_5$ in the 15 000 cm^{-1} regions) suitable for Coumarin 540 or Rhodamine 640 dye excitation. The ground multiplet is $^5I_8$ and the first excited multiplet $^5I_7$. For these five multiplets, there are 43 and 37 distinct crystal-field energy levels for Ho^{3+} ions located in sites of C_{4v} and C_{3v} symmetry, respectively.

A notation of a letter plus numerical subscript is adopted for labeling the crystal-field levels of various LSJ multiplets. The ground multiplet $^5I_8$ is labeled Z, with the ground state being Z_1, and the first excited multiplet $^5I_7$ labeled by Y. The levels of the close-lying $^5S_2$, $^5F_4$ multiplets are labeled E_1, E_2, etc. in order of increasing energy, and those of the $^5F_5$ multiplet by D_1, D_2, etc.

All the Ho^{3+} energy levels have wave functions necessarily transforming as one of the irreps of the appropriate point symmetry group for the Ho^{3+} ion site. For centers having Ho^{3+} ions in sites of C_{4v} symmetry, the energy levels transform as one of the five irreps γ_1–γ_5 of the C_{4v} point group, where the irreps γ_1–γ_4 are all of single dimension, while γ_5 is of double dimension. For centers having Ho^{3+} ions in sites of C_{3v} symmetry the energy levels transform as one of the three irreps γ_1, γ_2, or γ_3 of the C_{3v} point group, with γ_1 and γ_2 being of single dimension and γ_3 of double dimension. The predicted polarization ratios for C_{4v} and C_{3v} symmetry centers in both $\langle 100 \rangle$ and $\langle 111 \rangle$ polarization geometries have already been published,[4] while the corresponding ratios for the two possible varieties of low-symmetry C_s centers [shown in Figs. 1(b) and 1(c)] for the $\langle 100 \rangle$ polarization geometry are presented in Ref. 7. We reproduce a summarized version of the C_s symmetry tables in terms of the polarization character of the pump and fluorescence transitions (Table I), which provides polarization criteria for distinguishing the two low-symmetry centers. In all these tables, the various polarization geometries are specified by $x(ab)z$ in which x defines the direction of propagation of the incident laser beam, z is the direction of propagation of the analyzed fluorescence, $a(=y$ or $z)$ defines the polarization (electric vector) of the incident laser light and $b(=y$ or $x)$ defines the polarization of the fluorescence.

B. Laser-selective excitation and fluorescence spectra

Absorption spectroscopy is the most direct way of obtaining energy levels of the various rare-earth ion centers present. However, for Ho^{3+}, the absorption transitions to energy levels of the $^5S_2$ and $^5F_4$ multiplets are sufficiently weak to require Ho^{3+} concentrations above 0.02% in 10-mm thick CaF_2 crystals or 0.1% in 25-mm thick SrF_2 crystals to obtain well-defined absorption lines. In contrast, laser excitation gives good intensity spectra for Ho^{3+} concentrations down to 0.005% and is preferred for observing the very weak absorption lines of centers having relatively strong fluorescence. Such excitation spectra are obtained when the laser pump frequency is continuously scanned while monitoring the fluorescence. Either a spectrometer is tuned to a particular transition, specifically to record the excitation spectrum of the corresponding single center, or broadband wavelength selection is used to detect all fluorescing centers present. Laser excitation can have vastly superior sensitivity compared to absorption, but the observed line intensities are altered in accordance with the relative fluorescence efficiencies of the various centers present. Absorption spectra are still needed for observing the presence of any centers having very weak fluorescence compared to the major centers.

Fluorescence spectra from the $^5S_2$, $^5F_4$ (E), and $^5F_5$ (D) multiplets to various crystal-field levels of the $^5I_8$ and $^5I_7$ multiplets were recorded at 10 K and in some cases 2 K for the various Ho^{3+} centers, with selective excitation to the lowest appropriate absorption transition of the $^5S_2$ or $^5F_5$ multiplets. Such spectra were analyzed to obtain the energy-level schemes of the $^5S_2$, $^5F_4$, $^5F_5$, $^5I_7$, and $^5I_8$

TABLE I. Relative polarization intensities for C_s symmetry centers in $\langle 100 \rangle$-oriented crystals.

Pump transition	Decay transition	$C_s(a)$ $x(yy)z$	$C_s(a)$ $x(yx)z$	$C_s(b)$ $x(yy)z$	$C_s(b)$ $x(yx)z$
$\gamma_a \rightarrow \gamma_a$ [a]	$\gamma_a \rightarrow \gamma_a$	No restriction		No restriction	
	$\gamma_a \rightarrow \gamma_b$ [b]	$\frac{yx}{yy} \geq \frac{1}{2}$		0	1
$\gamma_a \rightarrow \gamma_b$	$\gamma_b \rightarrow \gamma_b$	$\frac{yx}{yy} \geq \frac{1}{2}$		0	1
	$\gamma_b \rightarrow \gamma_a$	2	1	1	0

[a] $\gamma_a = \gamma_1$ or γ_2.
[b] $\gamma_b = \gamma_2$ or γ_1.

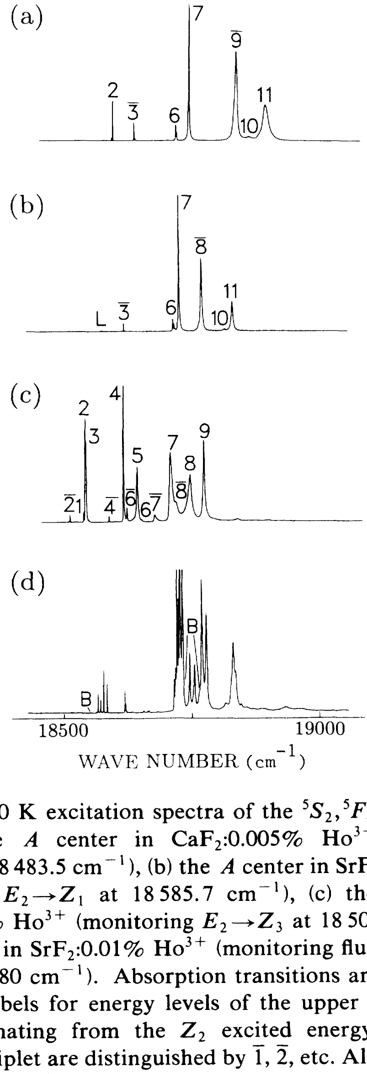

FIG. 2. 10 K excitation spectra of the $^5S_2$,$^5F_4(E)$ multiplet for: (a) the A center in CaF_2:0.005% Ho^{3+} (monitoring $E_1 \rightarrow Z_4$ at 18 483.5 cm^{-1}), (b) the A center in SrF_2:0.01% Ho^{3+} (monitoring $E_2 \rightarrow Z_1$ at 18 585.7 cm^{-1}), (c) the B center in CaF_2:0.005% Ho^{3+} (monitoring $E_2 \rightarrow Z_3$ at 18 504.5 cm^{-1}), (d) the B center in SrF_2:0.01% Ho^{3+} (monitoring fluorescence centered at 15 680 cm^{-1}). Absorption transitions are identified by numerical labels for energy levels of the upper (E) multiplet. Those originating from the Z_2 excited energy level of the ground multiplet are distinguished by $\bar{1}$, $\bar{2}$, etc. All transition energies are in cm^{-1} in air.

multiplets for each center studied.

The spectroscopy of the various centers is now discussed in turn.

1. The A center in CaF$_2$:0.005% Ho^{3+} *crystals*

Figures 2(a) and 3(a) include the excitation and fluorescence spectra of the A center present in CaF$_2$:0.005% Ho^{3+} crystals, observed by laser selective center discrimination.

The A center has two close-lying energy levels lowest, with the first excited level (Z_2) 1.9 cm^{-1} above the ground level. Detailed studies of this first excited-state energy interval under high resolution and by EPR have been previously reported[17,18] and the separation has been observed at 1.85±0.2 cm^{-1} in the far infrared absorption spectrum of a 48-mm thick CaF$_2$:0.05% Ho^{3+} crystal.[19]

The lowest energy level (E_1) of the $^5S_2$ multiplet was not observed in either absorption or excitation from the Z_1 or Z_2 energy levels. Its energy (18 599.0 cm^{-1}) was inferred from the observation of pairs of lines, separated by 14 cm^{-1}, for all the fluorescence transitions to γ_5-type energy levels of the Z and Y multiplets. The presence of this energy level was confirmed by the increase in intensity with temperature of all fluorescence transitions originating from the E_2 energy level at 18 613.2 cm^{-1}, indicating that this level is not the lowest energy level of the multiplet. Only transitions assigned as originating from the E_1 level were present in the 2 K spectra.

Transitions were not observed from either the Z_1 or Z_2 levels to the E_4 and E_5 levels of the $^5S_2$ and $^5F_4$ multiplets and the energies of these levels were identified, in spectra taken at temperatures up to 77 K, by the presence of additional fluorescence transitions from these particular E levels to the three γ_5 (Z_3, Z_5, and Z_{10}) energy levels of the ground $^5I_8$ multiplet (Fig. 4).

All the observed transitions of the A center measured in a ⟨100⟩-oriented crystal, were almost completely polarized, having polarization ratios close to the expected possible ratios of 1:0 and 0:1 for a Ho^{3+} site having C_{4v} symmetry when pumping a $\gamma_{a'} \rightarrow \gamma_{a'}$ ($a'=1$, 2, 3, or 4)-type transition.[4] The observed ratios clearly distinguish those fluorescence transitions involving γ_5 energy levels from those involving $\gamma_{a'}$ energy levels and establish the energy-level assignments presented in Table II. Likewise, all the transitions of the A center measured in ⟨111⟩-oriented crystals have polarization ratios in good agreement with those predicted for the ⟨111⟩ geometry[4] and confirm the energy-level symmetry assignments made.

Monitoring a $\gamma_{a'} \rightarrow \gamma_{a'}$ transition in the two possible analyzer positions gave polarized excitation spectra, which distinguished clearly the γ_5 symmetry levels of the upper multiplet from those of $\gamma_{a'}$ symmetry, for transitions originating from the same ground Z multiplet energy level.

Upconversion fluorescence was observed from the E ($^5S_2$,$^5F_4$) and F ($^5F_3$) multiplets for $Z \rightarrow D$ excitation. This fluorescence was weak, with the $E \rightarrow Z$ transitions being only 10^{-5} the intensity of those obtained by direct excitation of the E multiplet under similar excitation conditions.

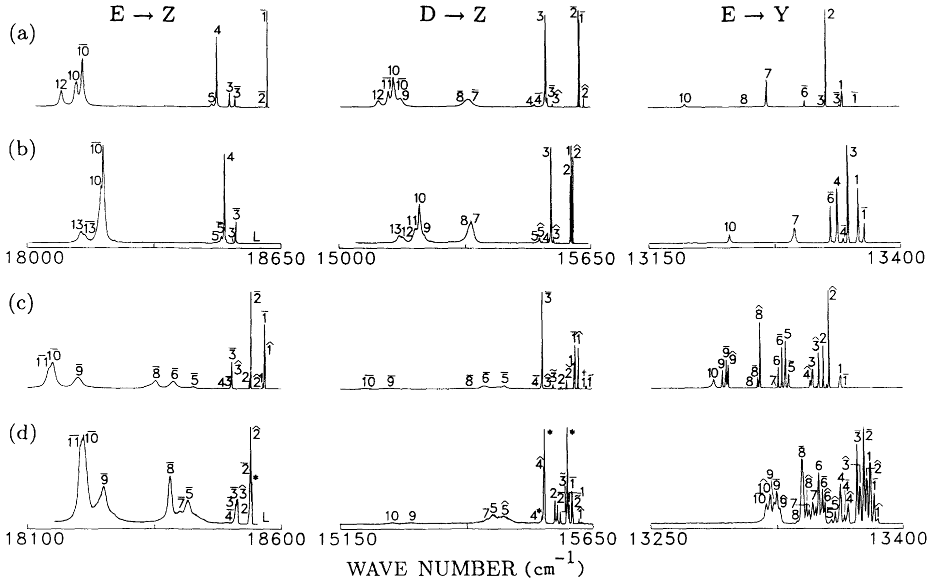

FIG. 3. 10 K fluorescence transitions $E \rightarrow Z$, $D \rightarrow Z$, and $E \rightarrow Y$ of: (a) the A center in CaF$_2$:Ho^{3+} (excitation $Z_2 \rightarrow E_9$ at 18 833.0 cm^{-1}), (b) the A center in SrF$_2$:Ho^{3+} (excitation $Z_1 \rightarrow E_2$ at 18 585.7 cm^{-1}), (c) the B center in CaF$_2$:Ho^{3+} (excitation $Z_1 \rightarrow E_4$ at 18 633.7 cm^{-1}), (d) the B center in SrF$_2$:Ho^{3+} (excitation $Z_1 \rightarrow E_2$ at 18 564.0 cm^{-1}). Assigned electronic transitions are identified by their terminating levels. Fluorescence transitions originating from higher energy levels E_2,E_3 of the E multiplet, and D_2, D_3 of the D multiplet are distinguished by ¯ and ^, respectively. Transitions identified by ˘, +, and ~ in 3(c) and (d) are from the D_4, D_5, and D_6 levels, respectively. Transitions identified by * in 3(d) are of an unidentified center. The position of the laser is shown by L. All transition energies are in cm^{-1} in air.

TABLE II. C_{4v} symmetry crystal-field fits to the $^5I_8$ (Z), $^5I_7$ (Y), $^5F_5$ (D), $^5S_2$ (E), $^5F_4$ (E), and $^5F_3$ (F) multiplets of the several C_{4v} symmetry centers identified in CaF_2:Ho^{3+}, SrF_2:Ho^{3+}, and related mixed crystals. All quantities are in cm^{-1} in air. Parameter values in parentheses are Er^{3+} values for comparison (see Sec. IV).

		CaF_2							SrF_2					
		A center		CS1 center		CB1 center			A center		SC1 center		SB1 center	
State	Symmetry	Calculated	Observed	Calculated	Observed	Calculated	Observed	Symmetry	Calculated	Observed	Calculated	Observed	Calculated	Observed
Z_1	γ_1	-2.3	0.0	-1.8	0.0	-2.7	0.0	γ_1	-3.1	0.0	-3.4	0.0	-1.1	0.0
Z_2	γ_2	-1.4	1.9	-0.1	2.0	-0.8	2.0	γ_2	-1.6	2.7	-1.8	2.5	1.0	2.5
Z_3	γ_5	84.6	83.0	70.3	70.0	64.5	63.5	γ_5	54.2	52.5	44.0	41.5	36.9	37.0
Z_4	γ_3	117.9	115.5	100.4	99.5	93.7	92.0	γ_3	79.2	75.5	65.7	61.0	54.7	54.0
Z_5	γ_5	133.7	128.0	118.8	115.0	111.5	107.5	γ_5	96.5	89.0	87.3	80.0	82.6	76.0
Z_6	γ_4	162.2	158.0	143.1		136.4		γ_4	119.4		108.4		97.2	91.0
Z_7	γ_1	288.0	284.5	296.0	296.0	297.4	296.0	γ_1	261.4	255.5	278.5	279.0	293.3	291.0
Z_8	γ_2	292.3	292.5	301.9	301.0	303.6	303.0	γ_2	266.2	265.5	283.8	282.0	300.9	305.0
Z_9	γ_3	450.1	455.0	441.5	441.5	434.8	433.5	γ_3	377.6	377.0	375.3	372.0	376.0	378.0
Z_{10}	γ_5	472.3	475.0	458.0	458.5	449.9	451.5	γ_5	389.8	393.0	386.7	389.0	382.4	383.5
Z_{11}	γ_1	494.5	492.0	474.6	473.0	465.7	464.5	γ_1	403.0	403.0	398.7	401.0	391.5	394.0
Z_{12}	γ_5	510.9	513.0	503.8	506.5	499.8	503.5	γ_4	429.2	430.0	430.9	430.0	431.9	430.0
Z_{13}	γ_4	512.1		499.3		491.4		γ_5	438.2	443.0	442.5	445.5	443.9	445.5
Y_1	γ_5	5255.6	5257.0	5252.7	5254.5	5248.0	5250.0	γ_5	5221.4	5220.5	5217.3	5217.0	5214.4	5215.5
Y_2	γ_3	5272.0	5273.0	5265.0	5266.5	5261.6	5262.0	γ_2	5222.8		5216.6		5212.5	
Y_3	γ_5	5270.2	5274.0	5268.7	5269.5	5269.6	5270.0	γ_3	5233.2	5231.0	5232.3	5231.5	5230.0	5230.5
Y_4	γ_2	5274.1		5257.8		5250.4		γ_5	5241.2	5241.5	5245.0	5246.0	5246.9	5245.5
Y_5	γ_4	5281.0		5278.9		5277.6		γ_4	5247.9		5249.6		5250.9	
Y_6	γ_1	5305.7	5308.5	5293.7	5295.0	5286.9	5289.0	γ_1	5252.7	5255.5	5247.9	5249.5	5247.5	5247.0
Y_7	γ_5	5333.2	5332.0	5323.4	5323.0	5319.8	5319.5	γ_5	5285.5	5283.5	5292.2	5289.0	5299.9	5305.0
Y_8	γ_3	5356.9	5355.0	5343.8	5345.0	5338.1	5337.5	γ_3	5301.4	5303.5	5300.7	5302.5	5301.4	5301.5
Y_9	γ_4	5406.9		5395.4		5388.3		γ_4	5341.9		5339.2		5340.5	
Y_{10}	γ_5	5416.7	5413.0	5402.6	5398.0	5394.8	5390.5	γ_5	5347.9	5348.5	5344.9	5345.0	5344.9	5341.5
Y_{11}	γ_2	5424.4		5409.0		5400.9		γ_2	5353.5		5350.2		5348.8	
D_1	γ_3	15606.1	15605.0	15601.8	15600.0	15599.8	15598.5	γ_5	15591.4	15593.0	15587.4	15590.0	15583.0	15588.0
D_2	γ_5	15609.2	15609.5	15603.0	15603.0	15599.7	15600.0	γ_3	15592.0		15591.0		15587.9	
D_3	γ_2	15623.3	15623.0	15614.0	15614.0	15608.7	15608.5	γ_2	15598.2	15599.0	15591.8	15594.5	15585.6	15593.0
D_4	γ_1	15673.1	15682.0	15660.8	15663.5	15653.3	15655.5	γ_1	15636.0	15642.3	15625.8	15630.0	15619.7	15624.0
D_5	γ_5	15756.8	15752.2	15761.8		15761.3		γ_5	15730.5	15727.8	15735.2	15735.4	15736.6	15733.6
D_6	γ_2	15759.6	15756.1	15766.3		15767.9		γ_2	15737.8	15735.1	15747.6	15742.4	15756.2	15750.5
D_7	γ_4	15771.7		15778.4		15778.6		γ_4	15746.0		15751.1		15757.3	
D_8	γ_5	15823.2	15823.5	15813.0		15806.8		γ_5	15766.9	15764.1	15769.0	15767.7	15770.4	15770.9
E_1	γ_3	18606.2	18599.0	18593.6	18590.0	18590.1	18586.0	γ_3	18582.6	18579.5	18578.6	18574.5	18575.6	18571.0
E_2	γ_1	18615.4	18613.2	18600.8	18601.0	18596.7	18596.6	γ_1	18586.4	18585.7	18582.1	18579.9	18578.6	18575.8
E_3	γ_5	18657.3	18655.1	18644.9	18646.6	18642.0	18644.1	γ_5	18624.0	18624.8	18624.2	18626.4	18623.8	18625.2
E_4	γ_4	18660.9	18666.5	18648.0		18645.1		γ_4	18627.6		18627.3		18626.5	
E_5	γ_3	18673.7	18681.5	18668.5		18669.0		γ_3	18664.5	18671.5	18668.9	18672.0	18671.4	18671.0
E_6	γ_5	18730.2	18726.8	18729.8	18725.6	18731.2	18728.2	γ_5	18722.6	18718.7	18726.1	18725.5	18728.4	18723.8
E_7	γ_1	18749.0	18750.1	18740.9	18744.3	18738.6	18743.0	γ_1	18724.4	18729.0	18719.6	18725.1	18715.6	18722.1
E_8	γ_4	18790.2		18790.9		18791.4		γ_2	18772.1	18771.0	18760.5	18757.2	18750.5	18747.8
E_9	γ_2	18833.1	18834.9	18805.2	18808.5	18794.6	18797.4	γ_4	18773.3		18780.3		18787.2	
E_{10}	γ_5	18859.5	18859.5	18848.1	18848.0	18844.7	18843.0	γ_5	18818.6	18817.5	18817.9	18817.3	18815.3	18815.0
E_{11}	γ_1	18889.6	18888.3	18872.0	18870.5	18866.3	18864.9	γ_1	18837.1	18833.7	18836.1	18831.0	18834.7	18829.1
F_1	γ_2	20741.0	20741.6	20727.3		20728.9		γ_2	20736.0	20735.5	20735.2	20736.0	20737.2	20737.0
F_2	γ_5	20780.6	20781.6	20754.5		20752.1		γ_5	20755.5	20756.5	20748.7	20750.0	20740.7	20746.0
F_3	γ_3	20846.1		20827.3		20828.2		γ_3	20823.5		20829.1		20828.4	
F_4	γ_4	20862.7		20851.2		20853.3		γ_4	20845.5		20849.8		20852.5	
F_5	γ_5	20925.9	20924.5	20901.6		20898.8		γ_5	20882.6		20879.8		20878.8	
Parameters														
B_A^2		685 (609)		508		428			338		235		153	
B_A^4		356 (409)		367		356			297		261		271	
B_A^6		419 (403)		376		370			325		287		229	
B_c^4		-1085 (-1172)		-1169		-1196			-1030		-1119		-1185	
B_c^6		557 (505)		557		556			488		502		509	
ζ		2139 (2390)		2143		2142			2139		2140		2141	
Number of levels fitted		39		30		30			36		36		37	
Standard deviation		3.9		2.6		2.8			3.7		3.6		4.2	

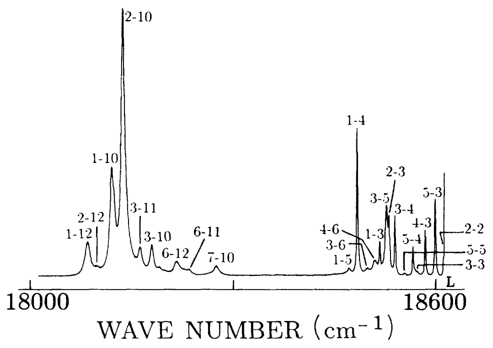

FIG. 4. 55 K fluorescence from the $^5S_2,^5F_4$ (E) multiplet of the A center in CaF_2:0.005% Ho^{3+} for excitation of the $Z_1 \rightarrow E_2$ transition at 18 613.2 cm^{-1} and with transition labeling showing both the upper- and lower-level identifications. The position of the laser is shown by L. All transition energies are in cm^{-1} in air.

2. The B center in CaF_2*:0.005%* Ho^{3+} *crystals*

Representative spectra are given in Figs. 2(c) and 3(c). The B center has the first excited crystal-field level (Z_2) 27 cm^{-1} above the Z_1 ground state. All levels expected for the E ($^5S_2,^5F_4$) and D ($^5F_5$) multiplets are observed, with the three lowest E levels (E_1, E_2, and E_3) and two lowest D levels (D_1 and D_2) having energy separations approaching the pump laser linewidth (Table III).

The fluorescence transitions of the B center in $\langle 100 \rangle$-oriented crystals show no intensity change in going from one polarization to the other, consistent with a center having Ho^{3+} ions in sites of trigonal (C_{3v}) symmetry. For $\langle 111 \rangle$-oriented crystals, well-defined polarization ratios of $\frac{3}{7}$ or $\frac{15}{11}$ are expected for many of the transitions when pumping $\gamma_{a'} \rightarrow \gamma_{a'}$ ($a'=1$ or 2)-type transitions.[4] For excitation of any of the $Z_1 \rightarrow E_1$, E_2, E_3, E_4, E_5, E_7, or E_9 transitions, the fluorescence transitions $E_1(\gamma_3)$, $E_2(\gamma_1)$, $E_3(\gamma_3) \rightarrow Z$ do not have any well-defined polarization, with most of the ratios being close to unity. Because of the small energy separation between the lowest three levels of the E multiplet, it appears that the measured ratios are a superposition of the polarizations of mixed transitions from the two close-lying γ_3 levels and the γ_1 level. In contrast, excitation of any of the $Z \rightarrow D_1$, D_2, D_3, D_5, or D_7 transitions yielded well-defined polarized $D_1, D_2 \rightarrow Z$ fluorescence transitions, whose ratios are fully consistent with a C_{3v} symmetry center assignment.

Upconversion fluorescence was not observed for the B center, giving an upper limit of 10^{-7} for the intensity of such fluorescence relative to that for direct excitation.

3. The CS1 and CS2 centers in 1% SrF_2 *in* CaF_2*:0.005%* Ho^{3+} *crystals*

Two additional centers (henceforth labeled $CS1$ and $CS2$) were identified in the spectra of CaF_2:0.005% Ho^{3+} crystals containing 1% SrF_2. Because the various absorption and fluorescence transitions of both these centers almost overlap with those of the A and B centers, it was possible to obtain their selective excitation spectra, completely discriminated from any lines of the A and B centers, only by monitoring fluorescence transitions from the respective lowest observable transition, $E_2 \rightarrow Z_1$ (Fig. 5).

Excitation and fluorescence spectra for the $CS1$ center were similar in both transition energies and polarization ratios to those of the A center (Figs. 5 and 6, and Table II). The energy-level separations of this center are all slightly smaller than those of the A center. The polarization ratios indicate a tetragonal C_{4v} site symmetry for the Ho^{3+} ion in this center, which is assigned as a C_{4v} center with a Sr^{2+} ion located on the C_4 symmetry axis on the opposite side of the charge-compensating interstitial F^- ion from the Ho^{3+} ion [Fig. 1(a)].

The $CS2$ center spectra differ from those of the $CS1$ center in having splittings of all the transitions corresponding to γ_5 doublet levels in C_{4v} symmetry centers (Figs. 5–7 and Table IV). These splittings indicate a Ho^{3+} site symmetry lower than C_{4v}. Possible low-symmetry centers that can be formed by the Sr^{2+} doping and involving just one nearby Sr^{2+} ion are those having a Sr^{2+} ion located in one of two different placings off the

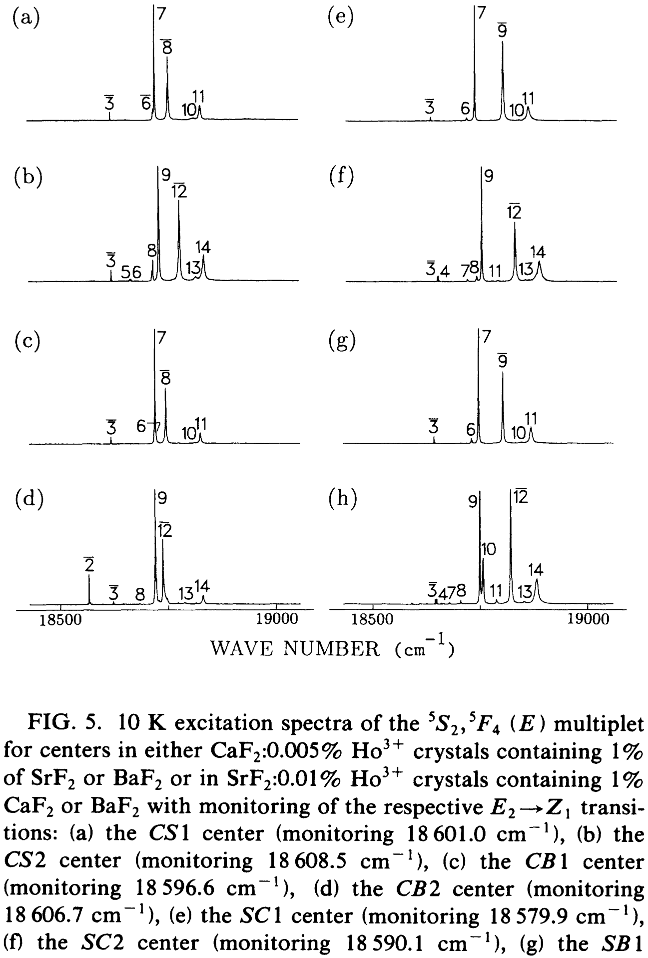

FIG. 5. 10 K excitation spectra of the $^5S_2,^5F_4$ (E) multiplet for centers in either CaF_2:0.005% Ho^{3+} crystals containing 1% of SrF_2 or BaF_2 or in SrF_2:0.01% Ho^{3+} crystals containing 1% CaF_2 or BaF_2 with monitoring of the respective $E_2 \rightarrow Z_1$ transitions: (a) the $CS1$ center (monitoring 18 601.0 cm^{-1}), (b) the $CS2$ center (monitoring 18 608.5 cm^{-1}), (c) the $CB1$ center (monitoring 18 596.6 cm^{-1}), (d) the $CB2$ center (monitoring 18 606.7 cm^{-1}), (e) the $SC1$ center (monitoring 18 579.9 cm^{-1}), (f) the $SC2$ center (monitoring 18 590.1 cm^{-1}), (g) the $SB1$ center (monitoring 18 575.8 cm^{-1}), (h) the $SB2$ center (monitoring a transition at 18 525.4 cm^{-1}). Transitions are identified by the upper multiplet level as in Fig. 2.

C_4 symmetry axis [Figs. 1(b) and 1(c)]. To distinguish which of these two models was appropriate to the *CS*2 center, the $Z_2 \rightarrow E_4$ transition at 18 650.8 cm^{-1} was pumped and the polarization ratios of the $E_1, E_2 \rightarrow Z_2, Z_4$ transitions measured. For these particular transitions, which are of $\gamma_1 \rightarrow \gamma_2$ type, distinctly different ratios of 0:1 or 2:1 are predicted[7] for the two model configurations. The polarization ratios observed are fully consistent with the model configuration of the center shown in Fig. 1(b).

There is still a choice of location of the Sr^{2+} ion relative to the Ho^{3+}-F$^-$ ion pair. As the *CS*2 center lines are close-lying satellites to those of the parent C_{4v} center, the effect of the Sr^{2+} ion is seen to be minor and only those centers having their Sr^{2+} ion lying closest to the Ho^{3+}-F$^-$ ion pair have a sufficiently perturbed Ho^{3+} ion site for their lines to be resolved from those of the parent C_{4v} center. All other mixed centers, with more remotely placed Sr^{2+} ions, would have their spectral lines wholly overlapped by those of the C_{4v} center, and other techniques, such as time resolution, would be needed to identify the presence of lines of such centers. Hence the mod-

TABLE III. C_{3v} symmetry crystal-field level fits to the $^5I_8$ (Z), $^5I_7$ (Y), $^5F_5$ (D), $^5S_2$ (E), $^5F_4$ (E), and $^5F_3$ (F) multiplets of the *B* center in CaF$_2$:Ho^{3+} and SrF$_2$:Ho^{3+}. All quantities are in cm^{-1} in air.

		CaF$_2$			SrF$_2$	
State	Symmetry	Calculated	Observed	Symmetry	Calculated	Observed
Z_1	γ_3	-2.9	0.0	γ_3	4.5	0.0
Z_2	γ_3	28.2	27.0	γ_3	20.6	26.5
Z_3	γ_1	64.5	65.0	γ_1	55.5	52.5
Z_4	γ_2	79.4	81.0	γ_2	67.8	70.0
Z_5	γ_3	144.5	138.5	γ_3	144.2	148.0
Z_6	γ_3	178.9	178.5	γ_2	158.8	
Z_7	γ_2	183.3		γ_3	167.6	163.0
Z_8	γ_1	214.1	213.5	γ_1	184.2	184.0
Z_9	γ_3	365.7	367.5	γ_3	313.5	315.0
Z_{10}	γ_3	413.6	417.5	γ_3	353.2	354.0
Z_{11}	γ_1	422.9	423.5	γ_1	361.4	359.5
Y_1	γ_3	5202.2	5202.5	γ_3	5184.7	5183.0
Y_2	γ_1	5216.2	5212.7	γ_2	5187.7	5189.0
Y_3	γ_3	5224.2	5218.9	γ_3	5196.0	5193.5
Y_4	γ_2	5221.1	5223.5	γ_1	5200.3	5200.5
Y_5	γ_3	5234.8	5235.3	γ_1	5211.8	5208.5
Y_6	γ_1	5237.8	5239.5	γ_2	5213.0	5214.0
Y_7	γ_2	5238.3	5240.9	γ_3	5217.5	5219.5
Y_8	γ_3	5252.5	5253.9	γ_3	5222.8	5226.0
Y_9	γ_3	5274.2	5272.9	γ_3	5241.2	5241.0
Y_{10}	γ_2	5282.2	5280.9	γ_2	5247.1	5247.0
D_1	γ_2	15608.4	15604.0	γ_2	15596.0	15595.5
D_2	γ_3	15606.0	15605.5	γ_3	15601.8	15601.5
D_3	γ_3	15613.2	15613.0	γ_2	15613.0	15615.5
D_4	γ_2	15617.8	15618.0	γ_3	15615.0	
D_5	γ_1	15629.9	15627.7	γ_3	15627.0	
D_6	γ_3	15631.7	15628.5	γ_1	15632.0	15630.5
D_7	γ_3	15649.0	15647.0	γ_3	15640.3	
E_1	γ_3	18566.4	18567.5	γ_1	18560.7	18561.6
E_2	γ_1	18566.8	18569.5	γ_3	18564.1	18564.0
E_3	γ_3	18569.6	18570.5	γ_3	18566.2	18565.6
E_4	γ_3	18627.9	18633.7	γ_3	18639.6	
E_5	γ_1	18654.9	18657.8	γ_1	18667.3	18666.7
E_6	γ_2	18657.4	18665.2	γ_2	18673.4	
E_7	γ_3	18717.4	18712.8	γ_3	18718.6	
E_8	γ_3	18750.9	18751.0	γ_3	18735.1	18736.5
E_9	γ_1	18772.3	18773.5	γ_1	18767.8	18767.2
F_1	γ_3	20718.8	20715.0			
F_2	γ_1	20719.9	20722.4			
F_3	γ_2	20751.1	20749.5			
F_4	γ_3	20780.4	20779.3			
F_5	γ_2	20802.9	20800.8			
Parameters						
B_A^2		197 (140.6)			52 (189.0)	
B_A^4		-72 (-76.7)			-184 (-246.8)	
B_A^6		-222 (-341.6)			-149 (-280.4)	
$\hat{B}_A^6$		-676 (-530.7)			-526 (103.6)	
B_C^4		46 (82.8)			-58 (1113.0)	
B_C^6		681 (581.0)			605 (986.7)	
ζ		2140 (2593.5)			2136 (2578.0)	
Number of levels fitted		41			30	
Standard deviation		3.3			2.9	

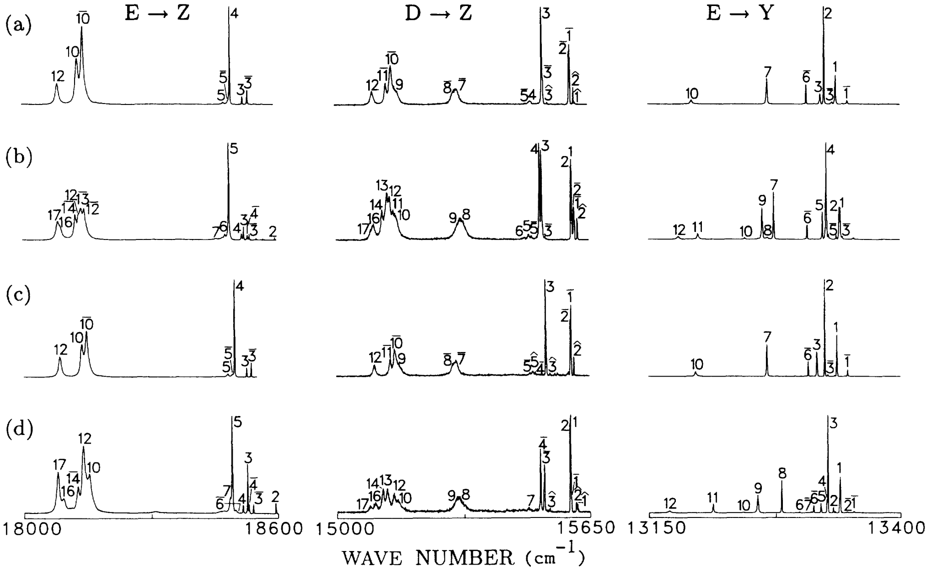

FIG. 6. 10 K fluorescence transitions $E \rightarrow Z$, $D \rightarrow Z$, and $E \rightarrow Y$ for centers in CaF_2:0.005% Ho^{3+} crystals containing 1% of SrF_2 or BaF_2 for excitation of the respective $Z_1 \rightarrow E_2$ transition: (a) the *CS*1 center (excitation at 18 601.0 cm^{-1}), (b) the *CS*2 center (excitation at 18 608.5 cm^{-1}), (c) the *CB*1 center (excitation at 18 596.6 cm^{-1}), (d) the *CB*2 center (excitation at 18 606.7 cm^{-1}). All transitions are identified by the lower multiplet level as in Fig. 3.

el configuration of Fig. 1(b) is proposed as that most likely applicable to the *CS*2 center.

The model proposed is the same as that for the principal off-axis mixed center observed in 0.5% SrF_2 in CaF_2:0.05% Pr^{3+} crystals.[7]

4. *The CB1 and CB2 centers in 1%* BaF_2 *in* CaF_2*:0.005%* Ho^{3+} *crystals*

The excitation and fluorescence spectra of the two identified centers *CB*1 and *CB*2 (Figs. 5 and 6) are similar to those of the *CS*1 and *CS*2 centers, respectively. While the Z_1–Z_2 energy-level separation of 2 cm^{-1} is closely similar for both sets of centers, all other levels are slightly lower in energy for the *CB*1 and *CB*2 centers compared to the corresponding *CS*1 and *CS*2 centers (Tables II and IV).

The observed energy-level patterns show that the *CB*1 center has a C_{4v} symmetry Ho^{3+} site while the *CB*2 center has a Ho^{3+} site with lower than C_{4v} symmetry (Fig. 8). As for the case of the *CS*2 center, pumping the $Z_2 \rightarrow E_4$ transition of the *CB*2 center and monitoring the $E_1, E_2 \rightarrow Z_2, Z_3$ transitions was carried out to distinguish between the two possible C_s point symmetry model configurations. For the *CB*2 center, the observed polarization ratios are fully consistent with the same low-symmetry center model configuration as the *CS*2 center [Fig. 1(b)] with the closest possible juxtaposition of the off-axis Ba^{2+} ion and the Ho^{3+}-F^- ion pair.

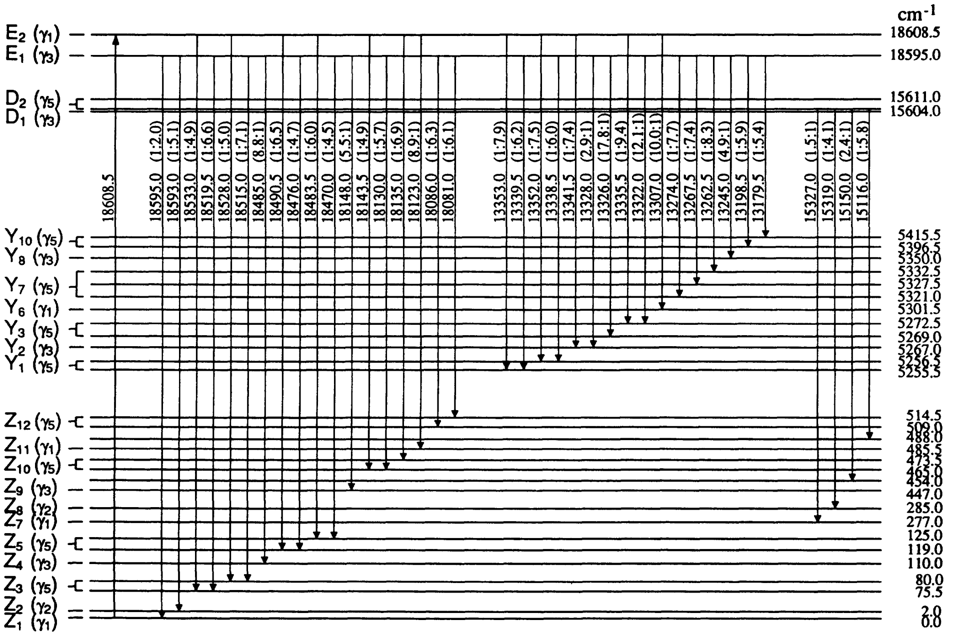

FIG. 7. Energy-level diagram for observed transitions of the *CS*2 center in CaF_2:0.005% Ho^{3+} showing measured transition energies (± 0.5 cm^{-1}) and $x(yy)z:x(yx)z$ polarization ratios ($\pm 5\%$). The energy-level assignments listed on the left are those of the parent C_{4v} center, while the *CS*2 center energy-level irreps themselves are presented in Table IV. For the particular Z levels not accessed by transitions from the E multiplet, the specific transitions from the D_1 energy level identifying them are shown.

5. *The A, B, SC1, SC2, and SB1 centers in* SrF_2*:0.01%* Ho^{3+} *crystals*

By laser-selective excitation, the excitation lines of five distinct centers were observed in SrF_2:0.01% Ho^{3+} crystals and these are so identified in Figs. 2 and 5. As for the mixed SrF_2 or BaF_2 in CaF_2 crystals, it was possible to obtain completely discriminated selective excitation spectra only by monitoring the $E_2 \rightarrow Z_1$ fluorescence transition in each case. The principal center has a close spectroscopic similarity to the *A* center in CaF_2 and is assigned as the analogous *A* center for SrF_2. Its polarization ratios for both the ⟨100⟩ and ⟨111⟩ polarization geometries and the crystal-field energy-level fit (see Sec. IV) all support this assignment. While the $Z_1 - Z_2$ energy-level separation of 2.7 cm^{-1} is larger than the 1.9 cm^{-1} found in the case of CaF_2, all the other levels lie closer together with, for example, the $E_1 - E_2$ energy-level separation being 6 cm^{-1}, compared to the 14 cm^{-1} for the *A* center in CaF_2.

Lines of the *B* center were found to have about 2% of the intensity of those of the *A* center and the spectral patterns are closely similar to those for the CaF_2 *B* center. Both the observed polarization ratios in the ⟨111⟩ polarization geometry for $D \rightarrow Z$ fluorescence with $Z_1 \rightarrow D_3$ excitation and the complete absence of any polarization for the ⟨100⟩-oriented crystals are consistent with a C_{3v} Ho^{3+} site symmetry in the *B* center.

Three other centers denoted here as *SC*1, *SB*1, and *SC*2 (Figs. 5 and 9) are spectroscopically related to the SrF_2 *A* center. SrF_2 crystals containing 1% CaF_2 have enhanced concentrations of the *SC*1 and *SC*2 centers and lower concentration of the *SB*1 center, whereas SrF_2 crystals containing 1% BaF_2 have the lines of the *SB*1

TABLE IV. Ho^{3+} energy levels (and their symmetry assignments) of the low-symmetry (C_s) mixed centers in 1% SrF_2 in CaF_2:0.005% Ho^{3+}, 1% BaF_2 in CaF_2:0.005% Ho^{3+} and 1% CaF_2 in SrF_2:0.01% Ho^{3+} crystals. All energies are in cm^{-1} in air.

	CS2 center		CB2 center		SC2 center	
State	**Symmetry**	**Level**	**Symmetry**	**Level**	**Symmetry**	**Level**
Z_1	γ_1	0.0	γ_1	0.0	γ_1	0.0
Z_2	γ_2	2.0	γ_2	2.0	γ_2	2.5
Z_3	γ_1	75.5	γ_2	69.0	γ_2	52.5
Z_4	γ_2	80.0	γ_1	79.5	γ_1	58.0
Z_5	γ_1	110.0	γ_1	105.5	γ_1	80.0
Z_6	γ_2	119.0	γ_2	103.5	γ_2	89.5
Z_7	γ_1	125.0	γ_1	110.0	γ_1	97.5
Z_8	γ_1	277.0	γ_1	283.0	γ_1	250.0
Z_9	γ_2	285.0	γ_2	293.5	γ_2	255.0
Z_{10}	γ_1	447.0	γ_1	442.5		
Z_{11}	γ_1	454.0				
Z_{12}	γ_2	465.0	γ_1	456.0	γ_1	390.0
Z_{13}	γ_1	473.5	γ_2	472.5	γ_2	396.5
Z_{14}	γ_1	485.5	γ_1	482.5	γ_1	409.0
Z_{15}	γ_2	488.0	γ_2	485.0		
Z_{16}	γ_1	509.0	γ_2	504.0	γ_1	439.0
Z_{17}	γ_2	514.5	γ_1	515.5	γ_2	445.5
Y_1	γ_2	5255.5	γ_1	5254.5	γ_2	5223.5
Y_2	γ_1	5256.5	γ_2	5261.0	γ_1	5226.0
Y_3	γ_2	5267.0	γ_1	5266.5	γ_1	5232.0
Y_4	γ_1	5269.0	γ_2	5267.5	γ_1	5241.0
Y_5	γ_1	5272.5	γ_1	5273.5	γ_2	5246.0
Y_6	γ_1	5301.5	γ_1	5295.0	γ_1	5260.5
Y_7	γ_2	5321.0	γ_2	5297.5	γ_1	5251.0
Y_8	γ_2	5327.5	γ_1	5312.5	γ_2	5285.0
Y_9	γ_1	5332.5	γ_2	5336.0		
Y_{10}	γ_1	5350.0	γ_1	5350.0	γ_1	5309.5
Y_{11}	γ_1	5396.5	γ_2	5380.5	γ_1	5314.0
Y_{12}	γ_2	5415.5	γ_1	5423.5	γ_2	5353.0
D_1	γ_1	15604.0	γ_1	15600.0	γ_1	15593.0
D_2	γ_2	15611.0	γ_2	15601.5	γ_2	15597.0
D_3			γ_1	15615.5	γ_1	15604.0
D_4	γ_2	15621.0	γ_2	15619.5	γ_2	15650.5
D_5	γ_1	15679.0	γ_1	15676.0	γ_1	15730.8
D_6					γ_2	15738.5
D_7					γ_2	15765.1
E_1	γ_1	18595.0	γ_1	18593.1	γ_1	18583.5
E_2	γ_1	18608.5	γ_1	18606.7	γ_1	18590.1
E_3	γ_2	18650.5	γ_2	18651.5	γ_2	18627.6
E_4	γ_1	18652.8	γ_1	18654.2	γ_1	18636.0
E_5	γ_2	18660.0	γ_2	18660.7	γ_2	18666.7
E_6	γ_1	18677.6	γ_1	18664.5	γ_1	18669.6
E_7	γ_2	18713.0	γ_1	18673.4		
E_8	γ_1	18736.4	γ_2	18704.1	γ_2	18718.9
E_9	γ_1	18748.2	γ_1	18746.6	γ_1	18734.0
E_{10}			γ_2	18753.4		
E_{11}	γ_2	18785.0	γ_2	18784.2	γ_2	18765.8
E_{12}	γ_2	18825.0	γ_1	18818.3	γ_2	18778.7
E_{13}	γ_1	18849.5	γ_2	18849.0	γ_1	18818.9
E_{14}	γ_1	18880.8	γ_1	18883.1	γ_1	18837.8

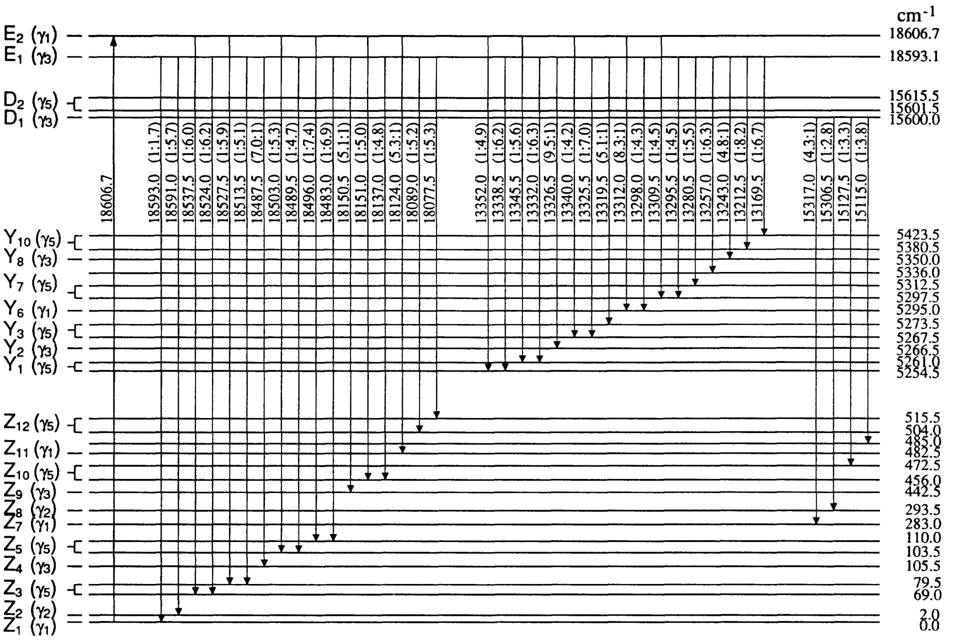

FIG. 8. Energy-level diagram for observed transitions of the *CB*2 center in CaF_2:0.005% Ho^{3+} showing measured transition energies and $x(yy)z:x(yx)z$ polarization ratios. Other details are as in Fig. 7.

center much stronger than those of the other two centers, together with those of a further center (labeled *SB*2). The lines of the latter center could not be successfully selectively separated as they are too close to those of the *SB*1 center. The centers *SC*1, *SC*2, and *SB*1 are, therefore, ascribed to the presence of small concentrations of Ca^{2+} and Ba^{2+} ions in the starting SrF_2 material. Similar crystals obtained from Optovac Inc. have these centers present at the same relative concentration at the same Ho^{3+} doping level.

By analogy with the *CS*1 center in mixed SrF_2 in CaF_2 crystals, the centers *SC*1 and *SB*1 are assigned as being C_{4v} symmetry centers with, respectively, a Ca^{2+} or Ba^{2+} ion lying on the Ho^{3+}-F^- axis [Fig. 1(a)].

As the *SC*2 center has splittings of those transitions corresponding to γ_5-type levels (Table IV) and its transitions have the same polarization behavior as the corresponding transitions of the *CS*2 and *CB*2 centers in mixed CaF_2 crystals (Fig. 10), it is assigned to the same model configuration as these centers [Fig. 1(b)].

The energy shifts of transitions of the mixed centers involving Ho^{3+} from those of the parent centers are sufficiently small to preclude observation of other varieties of possible mixed centers. In appropriate cases, these might be revealed by time resolution, as was done for the Pr^{3+} mixed centers.[7]

Upconversion fluorescence, of about 10^{-5} the strength of the more usual direct fluorescence, was observed from both the *E* and *F* multiplets for $Z \rightarrow D$ excitation of the *A*, *SC*1, or *SB*1 centers. The remaining *B*, *SC*2, and *SB*2 centers showed no upconversion fluorescence at all, setting an upper limit of 10^{-7} for the relative intensity of such fluorescence.

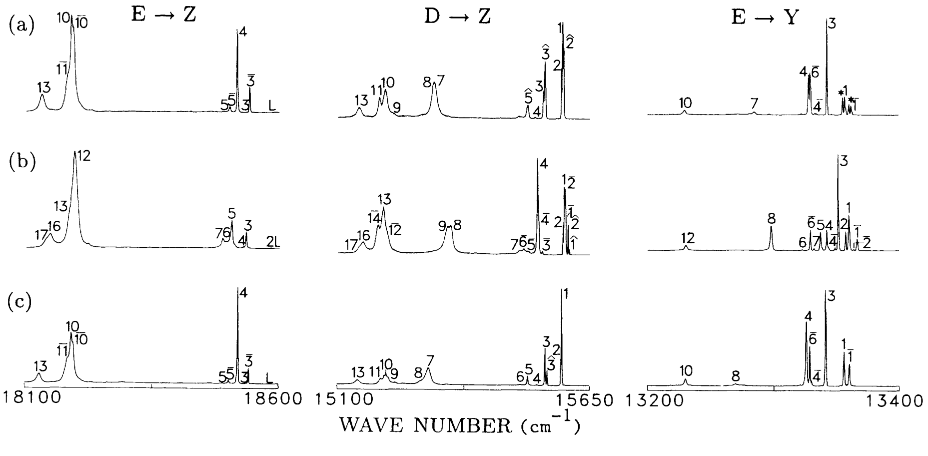

FIG. 9. 10 K fluorescence transitions $E \rightarrow Z$, $D \rightarrow Z$, and $E \rightarrow Y$ for centers in SrF_2:0.01% Ho^{3+} crystals containing 1% of CaF_2 or BaF_2: (a) the *SC*1 center (excitation $Z_1 \rightarrow E_2$ at 18 579.9 cm^{-1}), (b) the *SC*2 center (excitation $Z_1 \rightarrow E_2$ at 18 590.1 cm^{-1}), (c) the *SB*1 center (excitation $Z_1 \rightarrow E_2$ at 18 575.8 cm^{-1}). All transitions are identified by the lower multiplet level as in Fig. 3. The transitions identified by an asterisk in (a) are from the *SB*1 center.

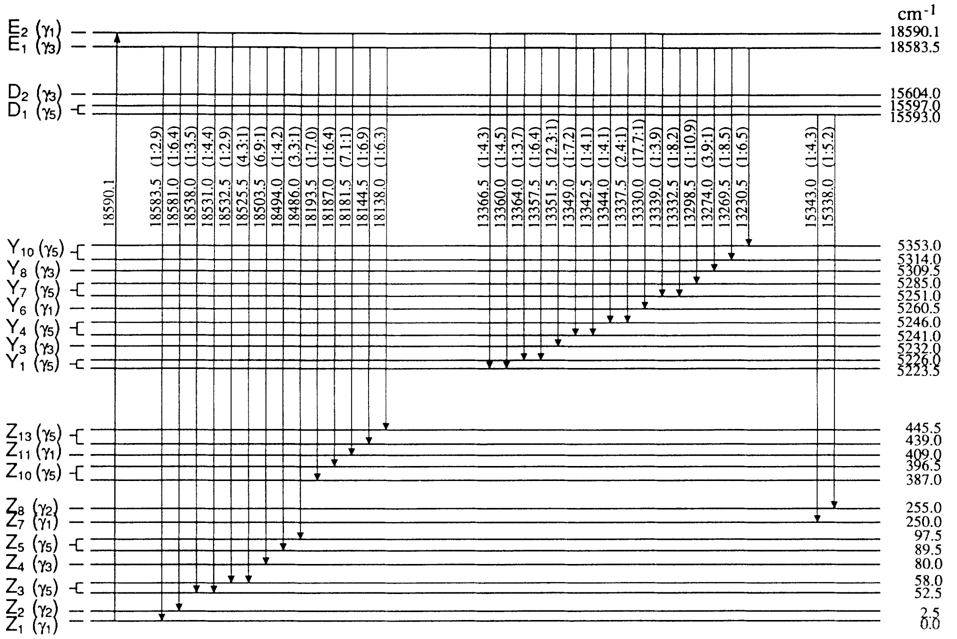

FIG. 10. Energy-level diagram for observed transitions of the *SC*2 center in SrF_2:0.01% Ho^{3+} showing measured transition energies and $x(yy)z:x(yx)z$ polarization ratios. Other details are as in Fig. 7.

IV. CRYSTAL-FIELD ANALYSES OF THE Ho^{3+} LEVELS IN C_{4v} AND C_{3v} SYMMETRY CENTERS

Crystal-field analyses were carried out to establish trends in the crystal-field parameters among the various centers of the same symmetry, to establish irrep labels for the many crystal-field levels, and to compare crystal-field parameters between different rare-earth ions.

The crystal-field Hamiltonian appropriate for C_{4v} symmetry is the same as that used for CaF_2:Er^{3+},[2] which, in terms of the Racah tensor operators $C_q^{(k)}$ has the form

$$\begin{aligned}H_{\text{cf}}={}&B_A^2C_0^{(2)}+B_A^4[C_0^{(4)}-\sqrt{\tfrac{7}{10}}(C_4^{(4)}+C_{-4}^{(4)})]\\&+B_A^6[C_0^{(6)}+\sqrt{\tfrac{1}{14}}(C_4^{(6)}+C_{-4}^{(6)})]\\&+B_C^4[C_0^{(4)}+\sqrt{\tfrac{5}{14}}(C_4^{(4)}+C_{-4}^{(4)})]\\&+B_C^6[C_0^{(6)}-\sqrt{\tfrac{7}{2}}(C_4^{(6)}+C_{-4}^{(6)})]\ .\end{aligned}$$

The chosen tensor combinations are the invariant scalars[20] in the point-group symmetry reduction chain $SO_3\rightarrow O\rightarrow D_4\rightarrow C_4$. The parameters of this Hamiltonian are linearly related to those used earlier[21] by the relationships

$$B_A^2=B_0^2\ ,$$

$$B_A^4=\tfrac{5}{12}B_0^4\ ,$$

$$B_A^6=\tfrac{7}{8}B_0^6\ ,$$

$$B_C^4=B^4+\tfrac{7}{12}B_0^4\ ,$$

$$B_C^6=B^6+\tfrac{1}{8}B_0^6\ .$$

For trigonal symmetry centers, the crystal-field Hamiltonian is identical to that used in the analysis of trigonal centers in CaF_2:Er^{3+} and SrF_2:Er^{3+} crystals.[3] The crystal-field fitting routine, supplied by Dr. M. F. Reid of the University of Hong Kong, was used for the crystal-field fits reported here. For each of the C_{4v} and C_{3v} assigned centers, the data from the crystal-field fits together with the proposed irrep labels are presented in Tables II and III.

The crystal-field parameters for the CaF_2 *A* and *B* centers are compared to those obtained for the corresponding centers in CaF_2:Er^{3+} by listing of the CaF_2:Er^{3+} crystal-field parameters,[3,21] expressed in the form adopted here, in parentheses in Tables II and III. The irrep label assignments listed for the various energy levels of the C_{4v} and C_{3v} centers are in agreement with the polarization data in all cases measured.

For the C_{4v} symmetry centers, the cubic crystal-field parameters are reduced slightly in going from CaF_2 to SrF_2, the second-degree axial crystal-field parameter B_A^2 decreases by about 50% and the higher-degree axial parameters by up to 25%. For the C_{3v} symmetry centers the cubic crystal-field parameters are again little altered, the second-degree axial parameter decreases by more than 70% and the higher-degree axial parameters vary with no clear-cut trend being apparent.

The substantial decrease in the second-degree axial crystal field is clearly manifested in the energy separations between the lower crystal-field levels of the measured multiplets, which, for the SrF_2 host, are typically half of those between the corresponding levels for the CaF_2 host.

The trend in crystal-field parameters in going from the parent C_{4v} centers to the C_{4v} symmetry mixed centers is almost solely a systematic decrease in the second-degree axial crystal-field parameter from the parent system values to progressively lower values in the Sr^{2+} and Ba^{2+} dopant cases. The other crystal-field paremeters change relatively little.

The main conclusions are that the Ho^{3+} ions in the various CaF_2 and SrF_2 C_{4v} symmetry centers experience an essentially unchanged cubic crystal-field environment, arising from the cubic arrangement of eight neighboring F^- ions and an altered axial crystal-field environment from displaced positionings of the charge-compensating F^- ion in the nearest-neighboring interstitial site. The whole center system in these fluorite crystals has recently been examined in detail by optically detected nuclear magnetic resonance (ODNMR) determinations of the F^- ion positions for the case of several parent and hydrogenic Pr^{3+} centers.[22]

V. FLUORESCENCE-LIFETIME MEASUREMENTS

The fluorescence decay times for emission from the *E* and *D* multiplets for the various centers obtained by direct excitation of the same multiplets are given in Table V. The fluorescence decay times for the CaF_2 *A* and *B* centers are in agreement with the earlier published data.[1] The fluorescence decay times of the corresponding transitions of the analogous *A* center in SrF_2 are factors of 1.4 and 3.7 longer for the *E* and *D* multiplets, respectively. These changes should relate to the decrease in the crystal-field parameters in going from CaF_2 to SrF_2 , but no simple relationship is apparent.

The mixed centers have lifetimes similar to their parent centers, with an overall decrease, apart from the exceptional case of fluorescence from the *E* multiplet for the *SB*1 center. In contrast, the Pr^{3+} mixed centers[7] showed, in most cases, longer lifetimes compared to those of the parent centers, and for the Pr^{3+} system the energy-level and crystal-field parameter changes are more pronounced.

It would require quite detailed calculations of radiative transition probabilities to give any quantitative insight into the observed lifetime trends. Nonradiative processes[23] may also make a significant contribution. The mixed centers are sufficiently close to their parent centers to suggest that the differences in their particular fluorescence lifetimes are comparatively minor changes resulting from slightly modified transition probabilities for the different centers.

TABLE V. 10 K fluorescence lifetimes for several Ho^{3+} centers present in CaF_2:0.005% Ho^{3+} SrF_2:0.01% Ho^{3+}, and related mixed crystals for direct excitation of the respective multiplet.

Crystal host	Center	Lifetimes (μs) $E(^5S_2)$	$D(^5F_5)$
CaF_2	*A*	1328±27	73.1±0.7
	B	532±10	114±1
1% SrF_2 in CaF_2	*CS*1	1236±25	84.2±0.8
	*CS*2	1080±22	87.8±0.9
1% BaF_2 in CaF_2	*CB*1	1282±26	81.2±1.6
	*CB*2	1228±25	90.9±1.8
SrF_2	*A*	1863±37	270±5
1% CaF_2 in SrF_2	*SC*1	1314±26	263±5
	*SC*2	1611±32	286±6
1% BaF_2 in SrF_2	*SB*1	2363±47	248±5

VI. CONCLUSIONS

Polarized fluorescence and energy-level patterns yield possible model configurations for a total of 12 centers in CaF_2:Ho^{3+} and SrF_2:Ho^{3+} crystals. The observed site symmetry change in rare-earth doped SrF_2 crystals, from tetragonal to trigonal symmetry as one goes along the rare-earth series, is found to occur between holmium and erbium, which are adjacent ions in that series. The spectroscopic data and the proposed models have formed the basis for hole-burning and ODNMR studies recently carried out on these Ho^{3+} centers at the Australian National University, Canberra, Australia, from which the placement of the neighboring F^- ions in the various centers could be examined. These modified F^- ion positions follow those established in previous ODNMR work on Pr^{3+} mixed[24] and hydrogenic[22] centers and will be reported elsewhere. The study of mixed-crystal centers has clearly established the presence of a low level of alkaline-earth impurities in the nominally pure CaF_2 and SrF_2 material used in these studies and in such crystals grown by Optovac. This observation also suggests that the *N*1 and *N*2 centers previously reported in SrF_2:Er^{3+} (Refs. 3 and 16) are very likely Ca^{2+} and Ba^{2+} varieties of the *N*3 center. This could be confirmed by a study of appropriate Er^{3+}-doped mixed crystals.

ACKNOWLEDGMENTS

This research was supported by the University of Canterbury and the New Zealand Lottery Board through research grants. One of us (M.M.) wishes to thank the New Zealand Ministry of Foreign Affairs. We thank Dr. M. F. Reid of the University of Hong Kong for providing his crystal-field fitting program and R. A. Ritchie, C. Rowe, and W. G. Smith for technical assistance.

---

[1] M. B. Seelbinder and J. C. Wright, Phys. Rev. B **20**, 4308 (1979).

[2] N. J. Cockroft, D. Thompson, G. D. Jones, and R. W. G. Syme, J. Chem. Phys. **86**, 521 (1987).

[3] N. J. Cockroft, G. D. Jones, and R. W. G. Syme, J. Chem. Phys. **92**, 2166 (1990).

[4] R. J. Reeves, G. D. Jones, and R. W. G. Syme, Phys. Rev. B **46**, 5939 (1992).

[5] Some confusion exists in the literature regarding the *A* and *B* center symmetry assignments because of a typographical error on page 4310 of Ref. 1. An apparent correction appears in Z. Hasan, R. Danby, and N. B. Manson, J. Lumin. **40&41**, 397 (1988), and a switched symmetry assignment is present in Ref. 6.

[6] S. H. Tang, H. Y. Zhang, M. H. Kuok, and S. C. Kee, Phys. Status Solidi B **168**, 351 (1991).

[7] Khong Yoon Loong, Ph.D. thesis, University of Canterbury, 1991.

[8] M. R. Brown, K. G. Roots, J. M. Williams, W. A. Shand, C. Groter, and H. F. Kay, J. Chem. Phys. **50**, 891 (1969).

[9] B. Bleaney, P. M. Llewellyn, and D. A. Jones, Proc. Phys. Soc. London Sect. B **69**, 858 (1956).

[10] A. A. Antipin, I. I. Kurkin, L. D. Livanova, L. Z. Potvorova, and L. Ya Shekunj, Zh. Tekh. Fiz. **36**, 1118 (1966) [Sov. Phys. Tech. Phys. **11**, 821 (1966)].

[11] J. Sierro, Phys. Lett. **4**, 178 (1963).

[12] M. V. Ermin, R. K. Luks, and A. L. Stolov, Fiz. Tverd. Tela (Leningrad) **12**, 3473 (1970) [Sov. Phys. Solid State **12**, 2820 (1970)]; A. A. Antipin, M. P. Davydova, M. V. Ermin, R. K. Luks, and A. L. Stolov, Opt. Spektrosk. **33**, 673 (1972) [Opt. Spectrosc. (USSR) **33**, 372 (1972)].

[13] U. Ranon and A. Yaniv, Phys. Lett. **9**, 17 (1964).

[14] U. Ranon and K. Lee, Phys. Rev. **188**, 539 (1969).

[15] B. Lal and D. Ramachandra Rao, Indian J. Phys. **54B**, 84 (1980).

[16] M. D. Kurz and J. C. Wright, J. Lumin. **15**, 169 (1977).

[17] L. S. Kornienko and A. O. Rybaltovskii, Fiz. Tverd. Tela (Leningrad) **13**, 2131 (1971) [Sov. Phys. Solid State **13**, 1785 (1972)].

[18] Z. Hasan, Solid State Commun. **73**, 109 (1990).

[19] J. A. Campbell (private communication).

[20] M. F. Reid and P. H. Butler, J. Phys. C **15**, 4103 (1982).

[21] C. A. Freeth and G. D. Jones, J. Phys. C **15**, 6833 (1982).

[22] N. B. Manson, Z. Hasan, P. T. H. Fisk, R. J. Reeves, G. D. Jones, and R. M. Macfarlane, J. Phys.: Condens. Matter **4**, 5591 (1992).

[23] L. A. Riseberg and H. W. Moos, Phys. Rev. **174**, 429 (1968).

[24] Khong Yoon Loong (private communication).

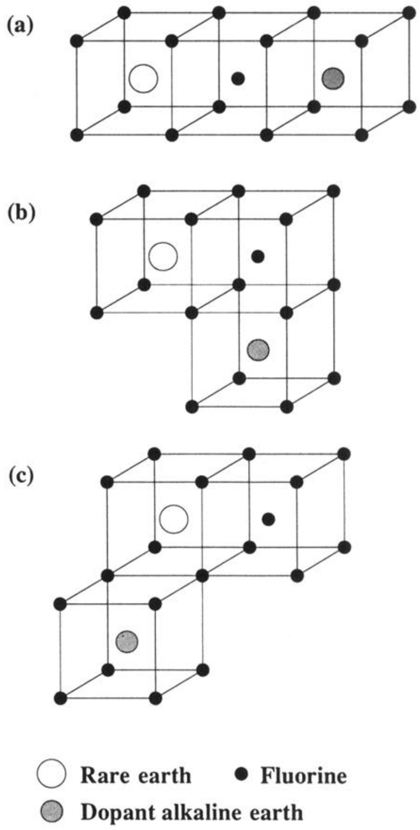

FIG. 1. Proposed modified C_{4v} center configurations obtained by introduction of a different alkaline-earth cation in the configuration of the regular C_{4v} center. (a) The on-axis modified C_{4v} symmetry center, (b) the off-axis (100) plane C_s symmetry center, and (c) the off-axis (110) plane C_s symmetry center.